Development of cosmic x-ray polarimeter

Asami Hayato, Toru Tamagawa, Naoko Tsunoda, Shigehira Hashimoto, Masao Miyamoto, et al.

Asami Hayato, Toru Tamagawa, Naoko Tsunoda, Shigehira Hashimoto, Masao Miyamoto, Mitsuhiro Kohama, Fuyuki Tokanai, Hideki Hamagaki, Masahide Inuzuka, Hiromasa Miyasaka, Ikuya Sakurai, Kazuo Makishima, "Development of cosmic x-ray polarimeter," Proc. SPIE 6266, Space Telescopes and Instrumentation II: Ultraviolet to Gamma Ray, 62663X (15 June 2006); doi: 10.1117/12.671242

SPIE.

Event: SPIE Astronomical Telescopes + Instrumentation, 2006, Orlando, Florida , United States

Development of cosmic X-ray polarimeter

Asami Hayato[a,b], Toru Tamagawa[b,a], Naoko Tsunoda[a,b], Shigehira Hashimoto[a,b], Masao Miyamoto[a,b], Mitsuhiro Kohama[a], Fuyuki Tokanai[d], Hideki Hamagaki[e], Masahide Inuzuka[f],Hiromasa Miyasaka[g], Ikuya Sakurai[h], Kazuo Makishima[c,b]

[a] Tokyo University of Science, 1-3 Kagurazaka, Shinjyuku-ku, Tokyo 162-8601 Japan;
[b] RIKEN, 1-2 Hirosawa, Wako, Saitama 351-0198, Japan;
[c] University of Tokyo, 7-3-1 Hongo, Bunkyo-ku, Tokyo 113-0033, Japan;
[d] Yamagata University, 1-4-12 Kojirakawa, Yamagata 990-8560, Japan;
[e] Center for Nuclear Study (CNS), University of Tokyo, 1-2 Hirosawa, Wako, Saitama 351-0198, Japan;
[f] National Research Institute for Cultural Properties, Tokyo, 13-43 Ueno Park, Taito-ku, Tokyo 110-8713 Japan;
[g] Caltech, MC 220-47, Pasadena, CA 91125, USA;
[h] Nagoya University, Furo-cho, Chikusa, Nagoya, Aiti 464-8603, Japan

ABSTRACT

We present a performance study of a cosmic X-ray polarimeter which is based on the photoelectric effect in gas, and sensitive to a few to 30 keV range. In our polarimeter, the key device would be the 50 μm pitch Gas Electron Multiplier (GEM). We have evaluated the modulation factor using highly polarized X-ray, provided by a synchrotron accelerator. In the analysis, we selected events by the eccentricity of the charge cloud of the photoelectron track. As a result, we obtained the relationship between the selection criteria for the eccentricity and the modulation factors; for example, when we selected the events which have their eccentricity of > 0.95, the polarimeter exhibited with the modulation factor of 0.32. In addition, we estimated the Minimum Detectable Polarization degree (MDP) of Crab Nebula with our polarimeter and found 10 ksec observation is enough to detect the polarization, if we adopt suitable X-ray mirrors.

Keywords: X-ray, Polarimeter, Polarization, GEM, Gas Electron Multiplier, Proportional Counter

1. INTRODUCTION

To detect polarization of cosmic X-rays provides us with very useful information which we have not succeeded to measure so far;[1] for example, 1) a detection of polarization of synchrotron X-rays makes it possible to measure magnetic fields in the objects because the synchrotron radiation is linearly polarized to the direction perpendicular to the magnetic fields. 2) polarization of reflected X-rays by an accretion disk has information of an inclination of the disk since the polarization of the X-ray is parallel to the inclination. However, detection of X-ray polarization has been limited by technologies. It is the only *OSO-8* satellite that has observed X-ray polarization in 1976.[2–4] After that, there has been no significant detection until now.

2. PRINCIPLE OF POLARIZATION DETECTION

The most effective method to measure the X-ray polarization strongly depends on the X-ray energy. Bragg reflection is used for very soft X-ray[5] (less than 1 keV) and Compton scattering is used for hard X-ray[6] (<30 keV). In the present paper, we focus on the intermediate energy range, a few keV to ∼30 keV, in which the photoelectric effects play the most important role for the detection of X-ray polarization.

Further author information: (Send correspondence to A.H.)
A.H.: E-mail: hayato@crab.riken.jp, Telephone: +81 (0)48 462 4874
T.T.: E-mail: tamagawa@riken.jp, Telephone: +81 (0)48 467 9336

Space Telescopes and Instrumentation II: Ultraviolet to Gamma Ray, edited by Martin J. L. Turner, Günther Hasinger, Proc. of SPIE Vol. 6266, 62663X, (2006)
0277-786X/06/$15 · doi: 10.1117/12.671242

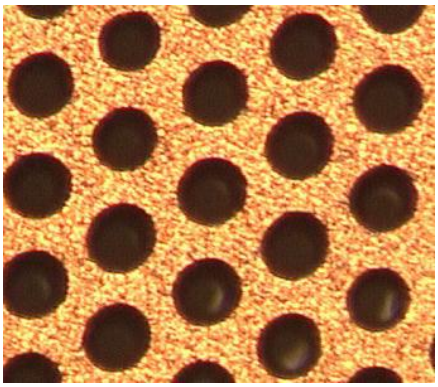

Figure 1. The micrography of the surface of the 50 μm-pitch GEM. It is laser etching processed and developed at RIKEN.

How to detect the polarization with the photoelectric effect is explained in the following. The scattering differential cross section of a photoelectron, which gives a possibility of a photoelectron moving into a certain solid angle $d\sigma$, is written as

$$\left(\frac{d\sigma}{d\Omega}\right)_p \propto \frac{\sin^2\theta\cos 2\phi}{(1-\beta\cos\theta)^4}. \tag{1}$$

In the equation θ is the angle between the direction of the photoelectron and that of the incident X-ray radiation. Due to the angular dependence of the cross section, photoelectrons are stochastically emitted to the polarized direction, when polarized X-rays are absorbed. Note that the definition of the polarization direction is the electric field direction of the incident X-rays. Therefore, we can measure the polarization of the incident X-rays with the determination of the photoelectron directions. Photoelectron tracks are better to be longer for tracing, so generally the gas is used as an X-ray absorber.[7–9]

3. GAS ELECTRON MULTIPLIER

In order to trace a photoelectron track in the gas, we have to measure the electron distribution which is produced by a photoelectron ionizing the gas. However, there is a significant problem; only few electrons are produced in a single X-ray absorption. Therefore, we have to multiple electron signal without losing position information. We make use of the Gas Electron Multiplier (GEM), which fully meets the requirement.

GEM had been developed at CERN in 1996.[10] A GEM is made of a polyimide foil, which is sandwiched by copper foils. There are a lot of holes in the foil with a pitch of $\sim$100μm. as shown in Figure 1. Electric fields are induced in those holes with applied the voltage applied to the copper foils of both sides. When a electron though a hole, it is accelerated by the field, and an electron avalanche is produced. As a result, the number of electrons are multiplied. A smaller hole pitch GEM was required for tracing a photoelectron, and the new laser etching technique has enabled us to develop a GEM with a 50 μm pitch.[11,12]

4. COSMIC X-RAY POLARIMETER

Figure 2 shows a concepts of our X-ray polarimeter. X-ray is absorbed by low Z noble gas mixture which fill the detector, then a photoelectron is emitted. The photoelectron takes its route with ionizing around gas atoms, so electrons are left along the photoelectron track. The electrons are drifted under-word due to the electric field produced by the drift plane. As soon as electrons reach the GEM, the number of electron is multiplied without losing their position information. After that, multiplied electrons are corrected by the underneath CMOS sensor, Acrorad/AJAT DIC-100T without a CdTe layer[13,14] (Figure 3). It is a fine pixelized (100 μm-pitch) electron reader. The usable area is 5×5 inch^2, but we used just 3/8 of the total in this time, which corresponds 252×381 pixels (2.52×3.81 cm^2). Finally we can obtain the photoelectron track as a charge distribution image.

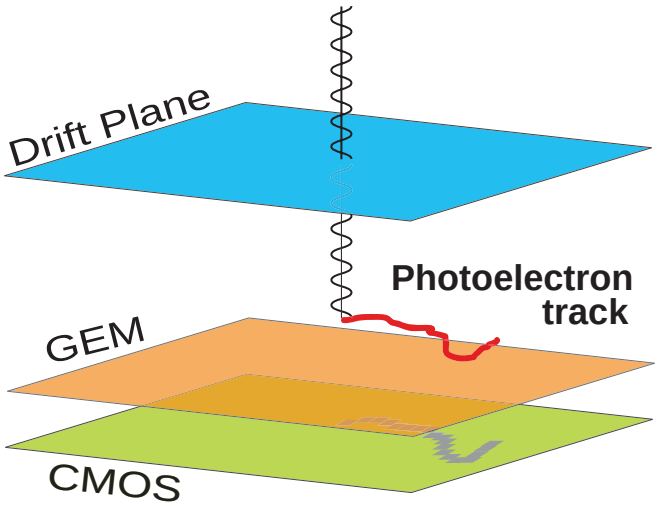

Figure 2. The concept of our X-ray polarimeter.

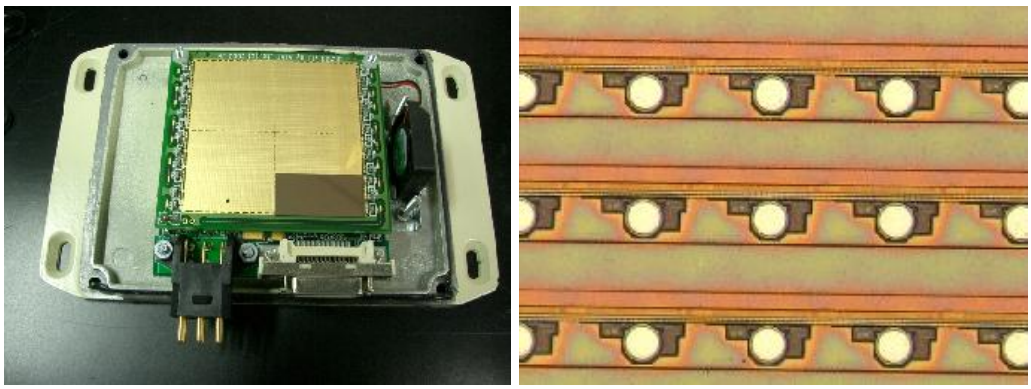

Figure 3. The top-view of the CMOS sensor (left). The right picture shows the micrography of the surface of the CMOS sensor. There are electrodes with the pitch of 100 μm.

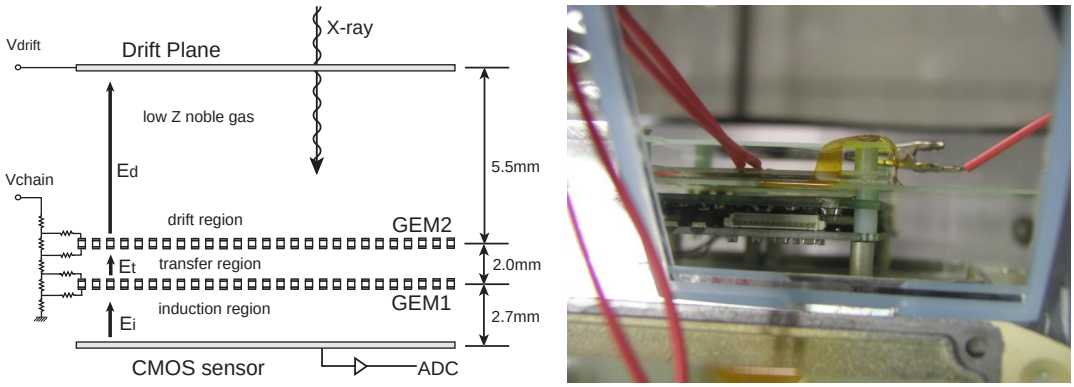

Figure 4. A schematic figure (left) and a picture (right) of the setup of the experiment.

5. PERFORMANCE STUDY

A performance study of our X-ray polarimeter has carried out. We evaluated the polarimetric sensitivity of our detector using highly polarized X-ray provided by a synchrotron accelerator at High Energy Accelerator Research Organization Photon Factory (KEK-PF[15]) in Japan.

5.1. Experimental Setup

The setup of the drift plane, the GEMs, and the CMOS sensor is shown in Figure 4. We used two 50 μm-pitch GEMs in the experiment, and those two were not aligned in position each other. We flowed Ne(80%)+CO_2(20%) into the polarimeter at 1 atmosphere. The applied voltage to each GEM was 420 V, and we had knew the electron gain reached about 4×10^3 in this condition by the previous calibration study. The electric fields in the drift region and the induction region were E_d=2.5 keV/cm and E_i=7.8 keV/cm respectively.

The X-ray beam energy was 10 keV in which was the intermediate energy the detector has sensitivity. The X-ray beam was polarized vertically. Since polarization degree of the X-ray beam, $P_{\rm beam}$, was unknown, it had been measured with another Compton polarimeter (Figure 5). The measured $P_{\rm beam}$ was 82% at 10 keV using a value of 0.94 as the modulation factor of the Compton polarimeter[16] .

We first set our polarimeter in 0 degree against the polarization direction and took the data for 1.5 ksec with the integration time of 0.02 sec (50 frames/sec). To study systematic effects, next we rotated the polarimeter -45 degrees clockwise as shown Figure 5 and the data were taken for another 1.5 ksec. We also took the data in 180 degree and 45 degree to compensate the systematic effects.

5.2. Data Analysis

5.2.1. Data reduction

We first summed up all pixel charges (ADCs) for each frame and made an ADC spectra (Figure 6). We found that the electron gain had changed about 10% of the total in few minutes. So, in order to select the frame in which a real single 10 keV event was, we made ADC spectra of every 1000 frames (20 seconds) and fitted the peak of frames which contained a single event with Gaussian function. Then we selected frames in the interval of the mean ADC $\pm$ 500 as event frames. After the reduction, about 15% of the total frames are left as event frames.

5.2.2. Determination of photoelectron emission direction

One of selected event frames is shown in Figure 7. We determined directions of photoelectron emissions of each event in based on Bellazzini et al. 2003,[17] but in this time, we did not find the reconstructed absorption point as they did. First we found the barycenter of the charge distribution as shown the crossed out in Figure 7 (right). We fixed the barycenter as the origin of the new coordinate system hereafter. Note that the barycentre

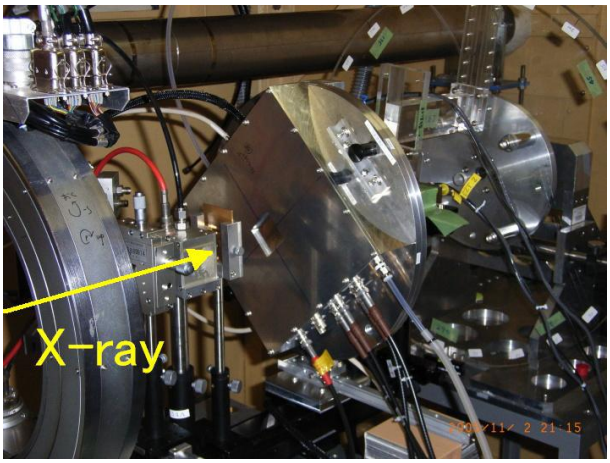

Figure 5. Setup picture of the polarimeter with the beam. The square box in the center of the picture is the detector. The behind acrylic circular board is the Compton polarimeter that is used for the beam calibration of polarization degree.

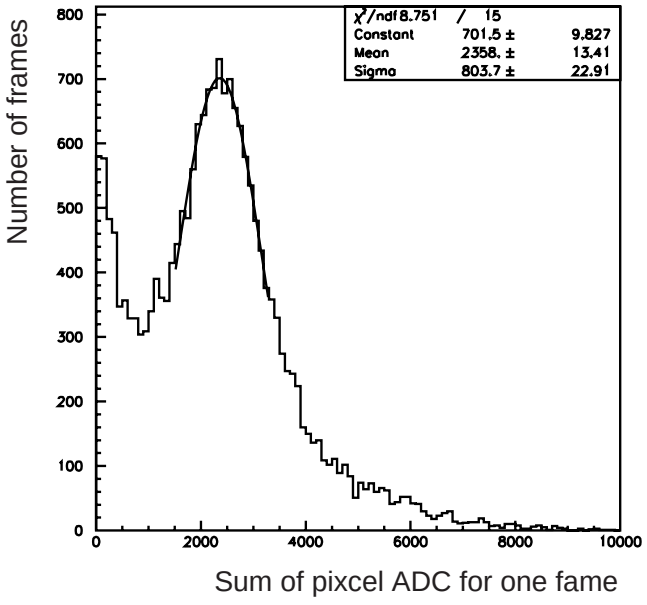

Figure 6. ADC spectrum. Note horizontal and vertical axis represents the sum of ADCs for a frame (not a event) and the number of frames (not events) respectively.

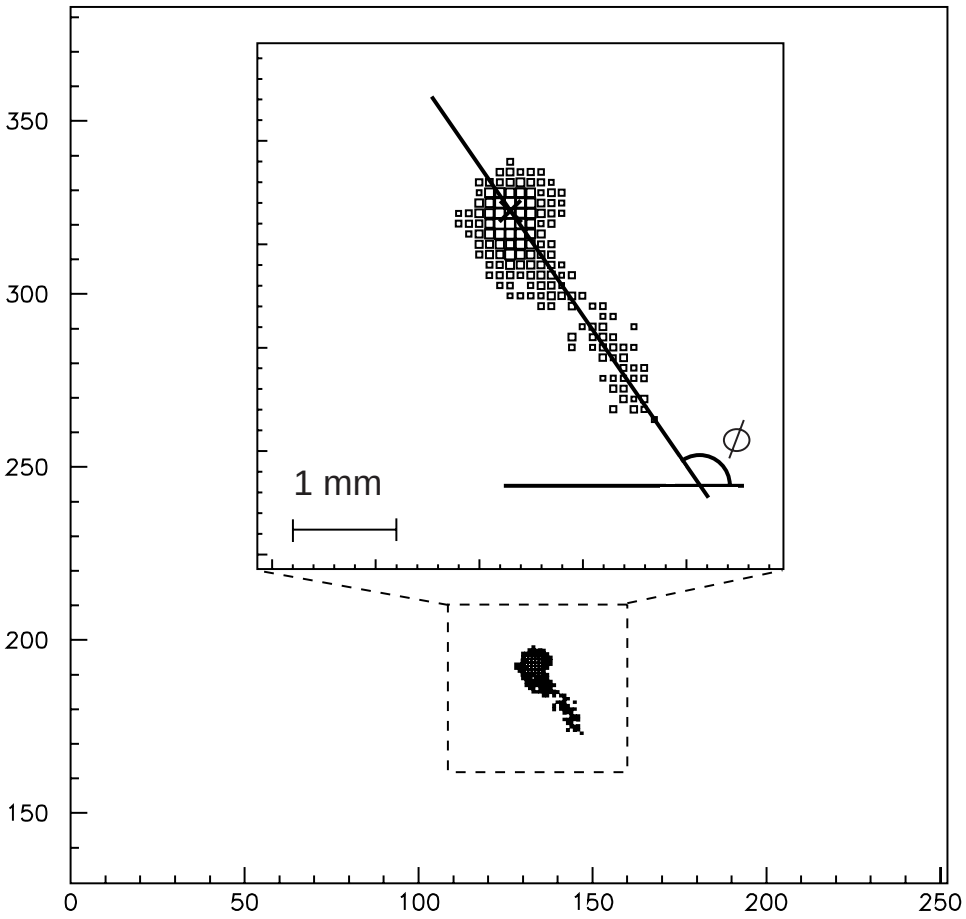

Figure 7. A single frame of the CMOS sensor with a close up of a single event image. The numbers indicate the pixel numbers of the CMOS sensor. The barycenter (cross), the principal axis, and ϕ are shown on the closed up photoelectron track, and ϕ is defined as the emission direction ϕ.

tend to be near the end of the tracks since the photoelectrons lose their energy right before they stop. Next, using an oriented angle from the original x axis ϕ, we calculated the second momentum M_2. Here we defined that two angels ϕ_{min} and ϕ_{max} as the angles give the minimum and maximum second momentum respectively. Those two angles within the interval $[-\pi,\pi]$ are obtained by setting the partial differential equation respect to ϕ of the second momentum is equal to 0. Obtained ϕ should be either ϕ_{min} or ϕ_{max}, and those two have to be perpendicular each other. In order to confirm either obtained ϕ is ϕ_{min} or ϕ_{max}, we substituted obtained ϕ and ϕ+90^o (or $\phi - 90^o$) into the second momentum equation. Finally we could find ϕ_{max} which gives the largest second momentum with respect to the barycenter. The ϕ_{max} and the principal axis are shown in Figure 7 (right). We defined ϕ_{max} as the direction of the photoelectron emission. At the same time, we calculated the eccentricity e of each photoelectron tracks which can be written as

$$\epsilon = \frac{M_2^{max}}{M_2^{min}} = \frac{1}{\sqrt{1-e}}. \tag{2}$$

We took up e for the next event reduction.

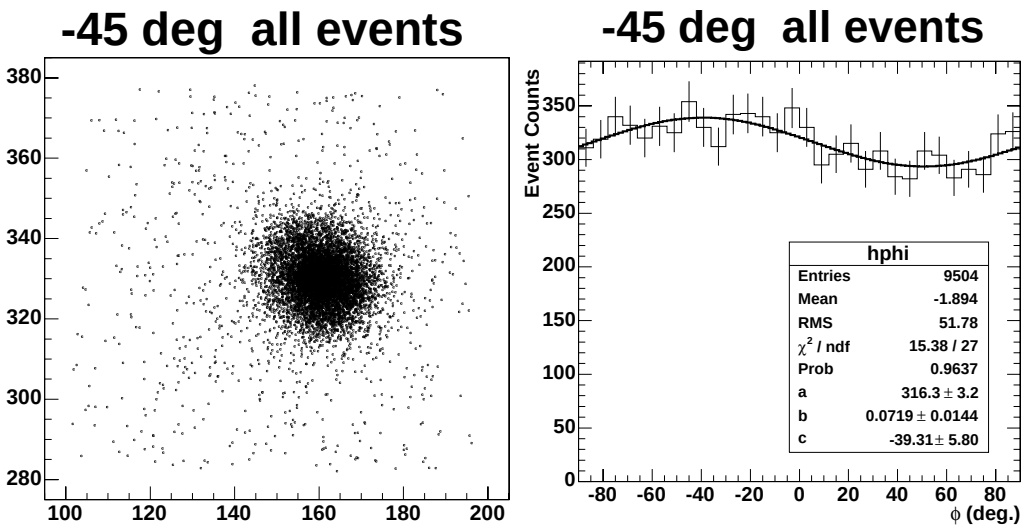

Figure 8. The barycentre distribution (left) and modulation (right) of all events. The expected polarization direction is -45 deg.

5.2.3. Modulation factor

Figure 8 shows the barycentre distribution (left) and the modulation (right) of all selected events. We fitted the moderation with the function of

$$f(x) = a + b\cos\left[2\left(x - c\right)\right]. \tag{3}$$

We can obtain the modulation factor of our polarimeter M with the following equation,

$$M = \frac{b}{aP_{beam}}. \tag{4}$$

Note that M is normalized with the polarization degree of the beam P_{beam}. As a result, the moderation factor was 0.09 when all events in -45 degree are selected.

Next we studied how the modulation factors change when we cut events with a certain e. As an example, Figure 9 shows the barycentre distributions (left) and modulation (right) of events with e>0.95. Because smaller e represents a shorter track event, it is reasonable that the events of their barycentore near the center of the distribution were reducted. In addition, it is easier to determine ϕ with events of lager e, so the modulation came to be better. The obtained moduration factor was 0.32 with $e > 0.95$ in -45 degree. This tendency is also shown in 0 degree (Figure 10 and Figure 11).

Figure 12 gives the number of left event frames and modulation factor within a cirtain e cut. Cuts in lager e makes modulation factor better, but excessive cuts make the factor's errors lager due to that the left events are few. The results of the modulation factors are different between in -45 degree and in 0 degree. We are considering that it caused by the square shape of the CMOS sensor pixel, and the studing is currently underway.

6. MINIMUM DETECTABULE POLARIZATION

A Minimum Detectable Polarization degree (MDP) is given with the following equation,

$$\mathrm{MDP} = \frac{n_\sigma}{\left(A\eta sT\right)M}\sqrt{2A\eta\left(s+b\right)T} \tag{5}$$

where n_σ is the lower confidence limits in σ, s and b are count rates (c s$^-$1) of the source and the background respectively. A is the effective area in cm^2, η is the efficiency, and T is the observation time in sec. We calculated

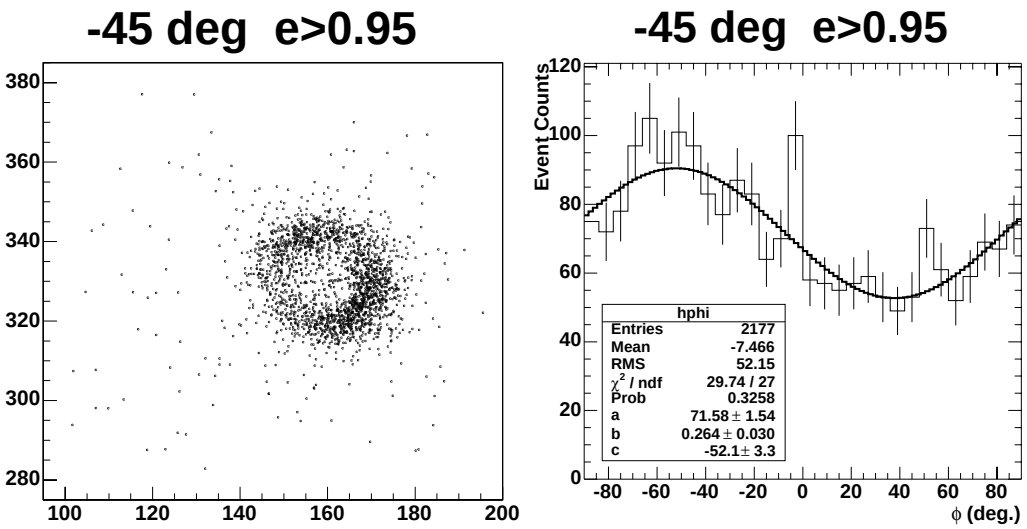

Figure 9. The barycentre distribution (left) and modulation (right) of events of their $e > 0.95$. The expected polarization direction is -45 deg.

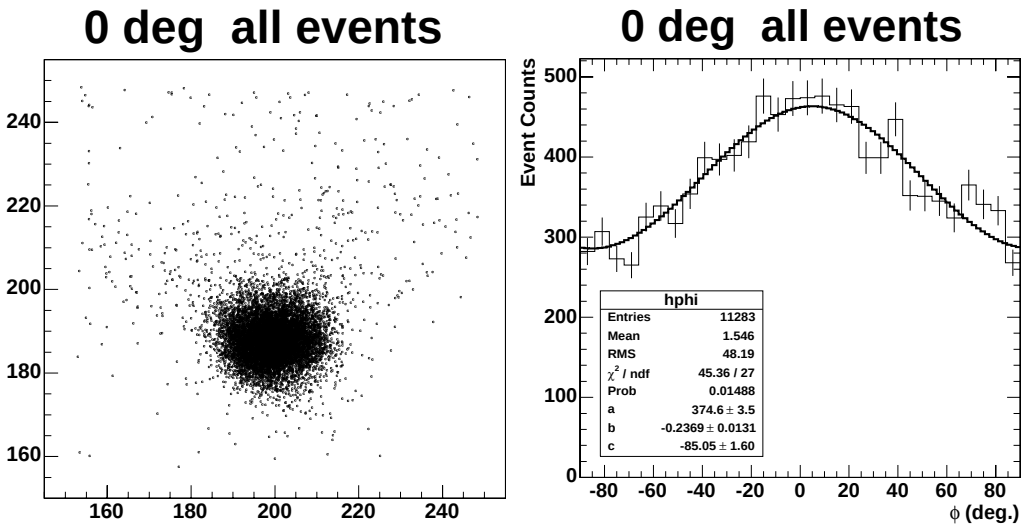

Figure 10. The barycentre distribution (left) and modulation (right) of all events. The expected polarization direction is 0 deg.

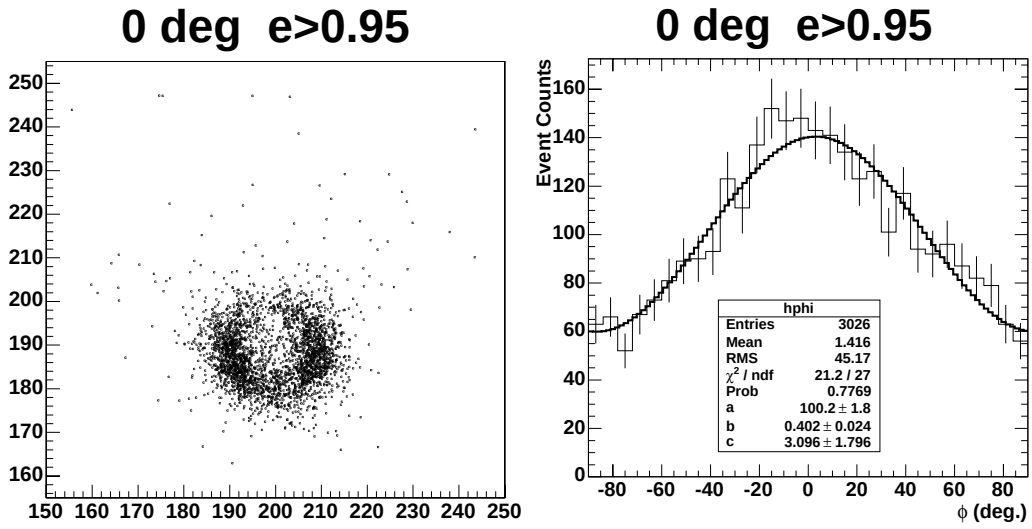

Figure 11. The barycentre distribution (left) and modulation (right) of events of their $e > 0.95$. The expected polarization direction is 0 deg.

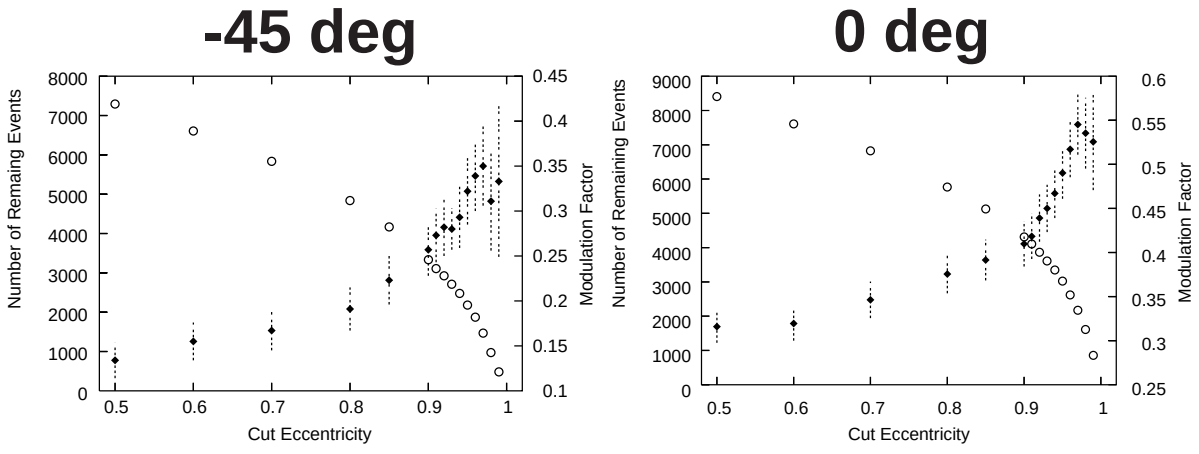

Figure 12. The holizontal axis signifies the cut eccentricity. The left and right vertical axes represent the number of events (Open CIrcles) and the modulation factors (diamonds) respectively. Plots are in −45 deg (left) and 0deg (right).

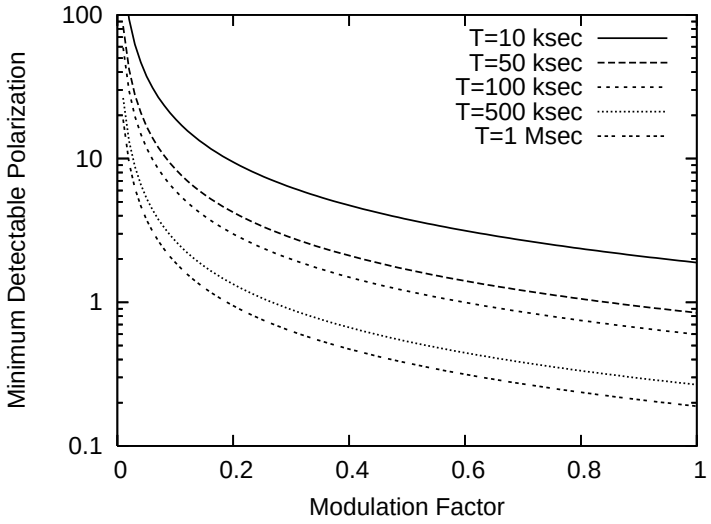

Figure 13. The relationship the modulation factor and the MDP for Crab Nebula in different observation time.

a MDP for Crab Nebula in the 2–30 keV band, in which our polarimeter is sensitive (Figure 13). Suppose to that the polarimeter is set at the focal plane of the *Suzaku* X-ray Telescope,[18] $A = 250$ cm^2. $\eta = 5{\times}10^3$ is estimated in consideration the kind of gas, its pressure, and its thickness. We used 3 for n_σ in this time. The count rate of the source[19] is 3.9 c s cm^{-2}, and it is large enough to neglect the background. As a result, we obtained the MDPs as shown in Figure 13. Using our polarimeter, the 10 ksec observation is enough to detect polarization of Crab.

7. SUMMARY

The performance study of a cosmic X-ray polarimeter, which based on the photoelectric effect in gas, has been carried out with the highly polarized X-ray provided by a synchrotron accelerator at KEK-PF in Japan. We have succeeded to obtain the image of the photoelectron track as the charge distribution with the 50 μm-pitch GEMs and the CMOS sensor. In the analysis, we have done the event selection by the eccentricity of the charge cloud of the photoelectron track. We finally obtained the relationships between the cut eccentricity and the modulation factor. For example, our polarimeter in -45 degree performed with the modulation factor of 0.32 by selecting the events of the eccentricity > 0.95. We also calculated the Minimum Detectable Polarization with our polarimeter in the case of the Crab Nebula observation, and we found it is possible to detect the Crab polarization with the only 10 ksec observation if we use the X-ray mirrors.

REFERENCES

1. E. Costa *et al.*, "Opening a new window to fundamentak physics and astrophysics: X-ray polarimetry," *Proc. 39th ESLAB Symposium*, pp. 19–21, 2005.
2. R. Novick, M. C. Weisskopf, R. Berthelsdorf, R. Linke, and R. S. Wolff, "Detection of X-Ray Polarization of the Crab Nebula," **174**, pp. L1+, May 1972.
3. M. C. Weisskopf, G. G. Cohen, H. L. Kestenbaum, K. S. Long, R. Novick, and R. S. Wolff, "Measurement of the X-ray polarization of the Crab Nebula," **208**, pp. L125–L128, Sept. 1976.
4. M. C. Weisskopf, H. L. Kestenbaum, K. S. Long, R. Novick, and E. H. Silver, "An upper limit to the linear X-ray polarization of Scorpius X-1," **221**, pp. L13–L16, Apr. 1978.
5. H. L. Kestenbaum, G. G. Cohen, K. S. Long, R. Novick, E. H. Silver, M. C. Weisskopf, and R. S. Wolff, "The graphite crystal X-ray spectrometer on OSO-8," *ApJ* **210**, pp. 805–809, Dec. 1976.

6. K. Hayashida, T. Mihara, S. Gunji, and F. Tokanai, "Hard x-ray polarimter for small satellite: design, feasibility study, and ground experiments," in *Polarimetry in Astronomy*, *Proc. SPIE* **5501**, p. 44, 2004.
7. R. Bellazzini and G. Spandre, "MicroPattern Gas Detectors with pixel read-out," *Nuclear Instruments and Methods in Physics Research A* **513**, pp. 231–238, Nov. 2003.
8. R. Bellazzini, F. Angelini, L. Baldini, F. Bitti, A. Brez, F. Cavalca, M. Del Prete, M. Kuss, L. Latronico, N. Omodei, M. Pinchera, M. M. Massai, M. Minuti, M. Razzano, C. Sgro, G. Spandre, A. Tenze, E. Costa, and P. Soffitta, "Gas Pixel Detectors for X-ray Polarimetry applications," *ArXiv Astrophysics e-prints* , Dec. 2005.
9. L. Baldini, F. Angelini, R. Bellazzini, F. Bitti, A. Brez, L. Latronico, M. M. Massai, M. Minuti, N. Omodei, M. Razzano, C. Sgro, G. Spandre, E. Costa, P. Soffitta, and L. Pacciani, "A gas pixel detector for x-ray polarimetry," *Nuclear Physics B Proceedings Supplements* **150**, pp. 358–361, Jan. 2006.
10. F. Sauli, "Gem: A new concept for electron amplification in gas detectors," *Nucl. Instrum. Meth.* **A386**, pp. 531–534, 1997.
11. T. Tamagawa, N. Tsunoda, A. Hayato, H. Hamagaki, M. Inuzuka, and H.Miyasaka, "Development of gas electron multiplier foils with a laser etching technique," *Nucl. Instrum. Meth.* , 2006. In Press.
12. T. Tamagawa, A. Hayato, Y. Yamaguchi, H. Hamagaki, S. Hashimoto, M. Inuzuka, H. Miyasaka, and K. M. I. Sakurai, F. Tokanai, "Fine-pitch and thick gas electron multipliers for cosmic x-ray polarimeters," 6266-146, in this proceeding.
13. Acrorad Co., Ltd.: http://acrorad.co.jp/index_us.html.
14. AJAT Oy Ltd.: http://ajat.fi.
15. KEK-PF: http://pfwww.kek.jp/index.html.
16. F. Tokanai, H. Sakurai, S. Gunji, S. M. H. Toyokawa, M. Suzuki, K. Hirota, S. Kishimoto, and K. Hayashida, "Hard x-ray polarization measured with a compton polarimter at synchrotoron radiation facility," *Nucl. Instrum. Meth.* **A530**, pp. 446–452, 2004.
17. R. Bellazzini, F. Angelini, L. Baldini, A. Brez, E. Costa, G. Di Persio, L. Latronico, M. M. Massai, N. Omodei, L. Pacciani, P. Soffitta, and G. Spandre, "Novel gaseus X-ray polarimeter: data analysis and simulation," in *Polarimetry in Astronomy. Edited by Silvano Fineschi . Proceedings of the SPIE, Volume 4843, pp. 383-393 (2003).*, S. Fineschi, ed., pp. 383–393, Feb. 2003.
18. The Suzaku Technical Description: http://www.astro.isas.jaxa.jp/suzaku/research/proposal/ao1/suzaku_td/.
19. A. Toor and F. D. Seward, "The Crab Nebula as a calibration source for X-ray astronomy," *AJ* **79**, pp. 995–999, Oct. 1974.